Bulletin of the Seismological Society of America, Vol. 72, No. 6, pp. 2349-2367, December 1982

THE LEAF-SPRING SEISMOMETER: DESIGN AND PERFORMANCE

BY E. WIELANDT* AND G. STRECKEISEN #

ABSTRACT

A small vertical seismometer whose inertial mass is supported by a leaf spring has been developed as a replacement for conventional long-period (LP) seismometers. The mechanical sensor has a virtually infinite natural period and is operated in a force-balance feedback configuration with an overall response identical to that of a 20-sec LP seismometer. Main considerations in the design were economic production and efficient shielding against environmental disturbances. The sensor is thermally coupled to the ground and protected from atmospheric pressure variations by a vacuum bell. This allows increasing the useful gain at very long periods by two orders of magnitude compared to a standard LP seismograph. The instruments resolve ground noise at least from a 0.3- to 300-sec period (typically, from about 0.1 to 3000 sec) and have a dynamic range of 140 dB. Leaf-spring seismometers have been tested since 1976 as part of wideband, LP, and very LP seismographs. Matching horizontal sensors are also available. This paper discusses the design principles and the initial calibration, and presents test results and typical seismograms.

DEVELOPMENTS IN LONG-PERIOD (LP) SEISMOMETRY

Electromagnetic LP seismographs have been in use since the beginning of this century, and it is surprising how little their general appearance has changed since then (cf. Galitzin, 1914, Figures 96 and 97). Major improvements resulted from the use of elinvar springs, the invention of a spring geometry with a constant and long free period (LaCoste, 1934), and the development of gold-foil suspension galvanometers. The last significant improvement, the rigid environmental control of the seismometer in a pressure tank, was implemented in the high-gain long-period (HGLP) project (Savino *et al.*, 1972). This installation marks at the same time the end of the technical development of the electromagnetic seismograph. A more detailed account of earthquake seismograph development has recently been given by Melton (1981).

Since about 1960 the introduction of active electronic sensing and feedback permitted the construction of LP seismographs with much smaller mechanical receivers that could more efficiently be protected from environmental noise. The first instrument of this kind was a modified LaCoste-Romberg tidal gravimeter with a three-plate capacitor for displacement sensing and electrostatic force feedback (Block and Moore, 1966). Today, most existing very-long-period (VLP) seismographs still make use of the same principle (Agnew *et al.*, 1976; Nakanishi *et al.*, 1976). These instruments have an excellent resolution in the free-mode and tidal bands but cannot replace conventional seismometers because their dynamic range is too small and their short-period response insufficiently controlled.

Once the problem of LP resolution was solved, attempts were made to build wideband seismometers that would have the potential to record the whole spectrum of teleseismic signals. An effort by Block and Moore (1970) to overcome the mechanical limitations of the LaCoste-Romberg gravimeter with a quartz torsion

* Present address: Institute of Geophysics, Swiss Federal Institute of Technology, CH-8093 Zürich, Switzerland.
† Present address: G. Streckeisen & Co., Messgeraete, Buchsweg 17, CH-8400 Winterthur, Switzerland.

#

accelerometer was technically successful but did not result in an instrument simple enough for wide distribution. Several other, more conventional constructions have reached series production. Among these, we mention the Teledyne-Geotech borehole seismometer model 36000 developed for the SRO project (Peterson *et al.*, 1976), the miniature wideband sensor developed by Usher *et al.* (1978) on the basis of a Willmore MkIII short-period seismometer, and the triaxial electronic seismometer EDS-1 of Unterreitmeier *et al.* (1978). However, none of these instruments appears to be useful for free-mode recording.

Our intention was primarily to build a small one-component wideband seismometer that could replace the bulky conventional LP instruments. The most difficult part to manufacture in a LaCoste-type seismometer is the zero-length helical spring; we have replaced it with a rectangular leaf spring as described later in this paper. The feedback circuit was adopted from an earlier experimental seismometer (Wielandt, 1973; Wielandt and Mitronovas, 1975). It generates a strong differential feedback force that overdamps the mechanical sensor so that its response becomes flat to velocity over a wide-frequency band. A prototype leaf-spring sensor was ready in 1976 when the German wideband seismic array GRF (Harjes and Seidl, 1978) was under construction. It was tested there against a Sprengnether High-

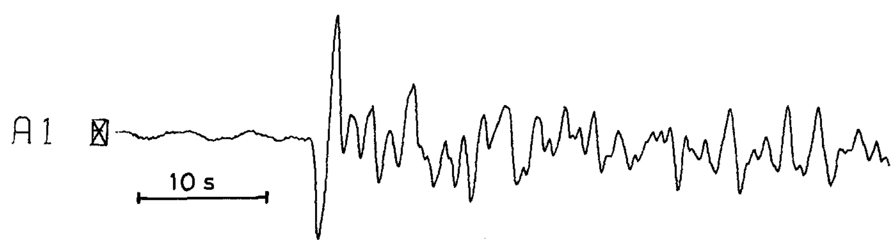

FIG. 1. Digital wideband records from a Sprengnether high-performance S-5100V seismometer and a prototype leaf-spring seismometer, plotted on top of each other. Only the superimposed station codes indicate that two signals were plotted. Earthquake in China on 15 November 1976 at 13:53 UTC. (Courtesy of D. Seidl, GRF Observatory.)

Performance S-5100V seismometer with digital recording in a passband from dc to 5 Hz and with a dynamic range of 132 dB. The records from the two instruments were visually identical (Figure 1; differences which exist between the instruments at very long periods cannot be seen in an unfiltered wideband record). The leaf-spring instrument was preferred for its smaller size and because it could be delivered precalibrated and ready for installation. An order of 18 instruments for the GRF array by the Deutsche Forschungsgemeinschaft initiated the commercial production and also the development of a matching horizontal seismometer of the "garden-gate" type.

At the time of writing, about 30 of the new vertical seismometers (Figure 2) and 20 horizontal ones are in service with a variety of recording characteristics: as wideband seismometers in the GRF array, as sensors of a telemetric HGLP network in Switzerland, and as wideband, LP, and VLP seismometers in other seismological observatories. The present paper reports mainly on the vertical instrument that has extensively been tested in the past 5 yr. The horizontal instrument appears to be of equal performance but requires an underground installation for a serious test. A suitable site is the Black Forest Observatory at Schiltach (West Germany) where a three-component set has been installed; results are to be published later.

The Cold Thermostat

The requirements for short-term temperature stability in a VLP seismometer are severe. Even if the mechanical system is compensated for slow variations of the temperature, it will exhibit a noticeable sensitivity to variations whose periods lie in the seismic band because its mechanical components have different thermal response times. The temperature coefficient of a mechanical sensor at seismic frequencies can hardly be smaller than a typical thermal expansion coefficient, say 10^{-5} per °C. If we want to resolve ground noise between 50- and 500-sec periods, at a level of roughly 10^{-11} (rms) of normal gravity, then we must avoid temperature

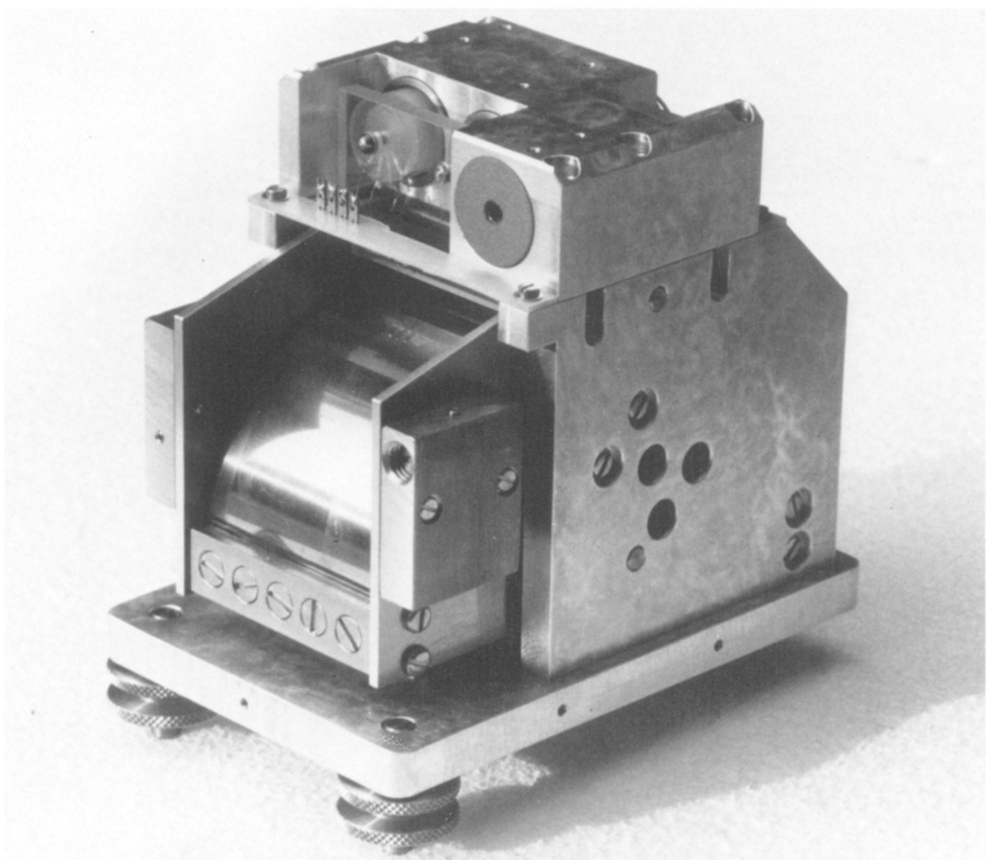

FIG. 2. The leaf-spring sensor with its cover removed. Outer dimensions with cover are approximately 18 × 18 × 12 cm.

fluctuations greater than 10^{-6} °C in that band of periods. Active temperature control with such a precision would be difficult to realize, but the thermal inertia of the sensor can provide the necessary short-term stability. The thermostat in gravimeter-type VLP instruments serves mainly to eliminate long-term temperature drift of the suspension which would otherwise saturate the displacement sensor or the feedback electronics within a short time. Due to its large dynamic range, the leaf-spring seismometer can be used as a VLP sensor without a thermostat provided that it is thermally coupled to the ground and well isolated against the ambient temperature. At the same time, the sensor must be protected from variations of the atmospheric air pressure; its seismic mass would otherwise experience a variable buoyant force at least three orders of magnitude larger than the seismic background noise, even under quiet weather conditions (Figure 3). The sensor must also be shielded from magnetic fields because all presently available temperature-compensated spring materials are ferromagnetic.

We install the sensor under a vacuum glass bell of 25 cm diameter resting on a glass plate that is cemented to the ground. Figure 4 illustrates the arrangement. The sensor has a massive aluminum cover to increase its thermal inertia and stands free inside the other shields. These comprise a Permalloy cylinder for magnetic

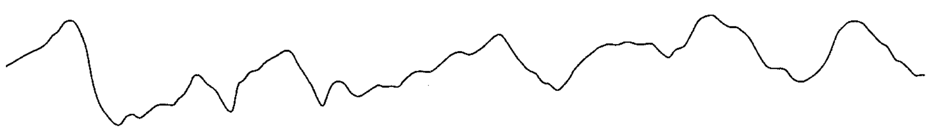

FIG. 3. VLP seismic traces from a completely shielded leaf-spring sensor, with the vacuum bell open (*top*) and sealed (*bottom*). The length of each trace is 75 min. This test indicates that variations of the atmospheric pressure must be suppressed at least by three orders of magnitude to become insignificant.

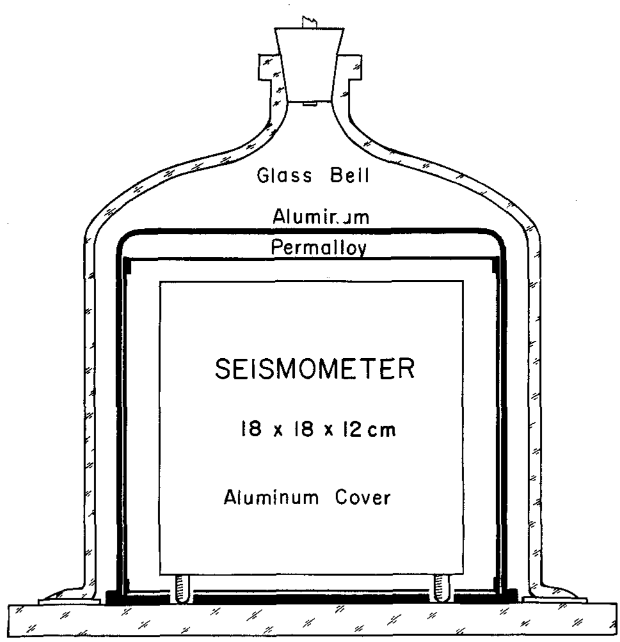

FIG. 4. Arrangement of the sensor and its shields inside the vacuum bell.

shielding and an aluminum container whose lower surface is cemented to the glass plate and, thus, in thermal contact with the ground. Electrical connections go through the silicone rubber fitting between the bell and the glass plate. The glass bell is evacuated to some 10 mbar, which is sufficient to suppress internal convection. The quality of the vacuum is not critical, and no later pumping is required. Fiber wool, heat reflecting blankets ("space blankets"), and a styrofoam cover provide additional isolation. Temperature changes in the seismic vault have no visible effect on the VLP record; however the instruments exhibit a slow seasonal drift and must be recentered a few times a year.

THE MECHANICAL SENSOR

The mechanical design of a LP seismometer lost much of its former significance when electronic sensing and feedback were introduced. While the maximum magnification of an electromagnetic seismograph is directly related to the size of its inertial mass, an electronic seismograph can have any desired gain. The magnification is only limited by the presence of environmental and instrumental noise. The inertial mass must, however, be chosen sufficiently large such that its thermal (Brownian) motion remains smaller than the seismic noise. The product of inertial mass, free period, and mechanical quality factor must exceed some minimum value in the order of 1 kg sec (see the section on "Instrumental Noise"). A minimum value of the free period is imposed by the relationship $\Delta g = \Delta x^* \, 4\pi^2/T^2$ (Melton and Kirkpatrick, 1970) which relates the acceleration resolution Δg at long periods to the free period T and the resolution Δx of the displacement transducer. For a resolution of $10^{-11}g$, possible combinations of T and Δx are: 10^{-8} m resolution at a free period of 60 sec, 10^{-10} m at 6 sec, and 10^{-12} m at 0.6 sec. Although it is an attractive idea to record LP seismic signals with a miniature instrument of a 0.6-sec free period, and both Block and Moore's quartz accelerometer and Usher's miniature, wideband sensors have demonstrated that such a construction is possible; the price that must be paid for the "elegant" solution is high. A displacement sensor whose resolution is in the order of 10^{-12} m necessarily has a very small range. It is difficult to test and calibrate and imposes severe restrictions on the feedback system that must keep the seismic mass within the range. We have, therefore, preferred to make the free period of the suspension as long as the available space permitted, and use a displacement transducer with a less extreme resolution. A resolution of 10^{-10} m (peak-to-peak) is sufficient for short-period teleseismic recording. To resolve ground noise at long periods, we then need a mechanical system with a free period of at least 6 sec.

Until recently, vertical LP siesmometers could only be realized with LaCoste-type suspensions. The use of a leaf-spring suspension for the same purpose has been suggested by different authors (Willmore, 1966; Jacoby, 1971; Unterreitmeier, 1974) but no practical results have been published. The restoring force of a LP seismometer suspension must not only be small but also constant; this implies that the first two derivatives of the elastic potential with respect to the mass position must vanish. Apparently, it has not been possible to satisfy these two conditions by trial and error. However, the mathematical analysis of the problem is difficult. A leaf spring under load assumes a shape described by elliptic integrals (Born, 1906) that cannot be solved explicitly for the geometric parameters. We use an originally flat leaf spring that assumes a roughly semi-circular shape under load. Our concept is, thus, in a way, similar to that of the 100-yr-old Gray Milne seismograph (Milne, 1888); however we do not provide an auxiliary period-lengthening device and have the spring clamped at both ends. Another similar construction dating from 1949 is reported by Melton (1981). To determine the geometrical parameters, the suspension was modeled numerically with a finite-element scheme. A systematic search revealed that useful LP suspensions can be derived from a variety of starting configurations by moving the spring clamps outward from the hinges such that the spring assumes a somewhat elongated shape. One of the many possible solutions was published earlier (Wielandt, 1976). Two prototype seismometers with that geometry were built; one of them is the instrument from which the noise spectrum in Figure 10 was obtained. For the commercial version, the spring geometry was modified in order to eliminate a parasitic resonance at 27 Hz. The new system (Figure 5) has a shorter and stiffer spring whose lowest resonance is at 80 Hz. Both suspensions have the desirable property that the restoring force has a minimum when the mass is centered; this assures that the mass will always return after a large deflection. As with the LaCoste suspension, the free period can be made virtually infinite and can be adjusted by tilting the whole instrument. In the feedback configuration, the mechanical free period is longer than 30 sec. We have not noticed any shortcomings of these leaf-spring suspensions against LaCoste suspensions in seismological applications.

Temperature Compensation

When the leaf spring is made from an elastically self-compensated material such as elinvar, the changes in spring geometry resulting from the thermal expansion of the frame cause a positive overall temperature coefficient (TC). An ordinary uncompensated spring material gives a strong negative TC. With two parallel strips

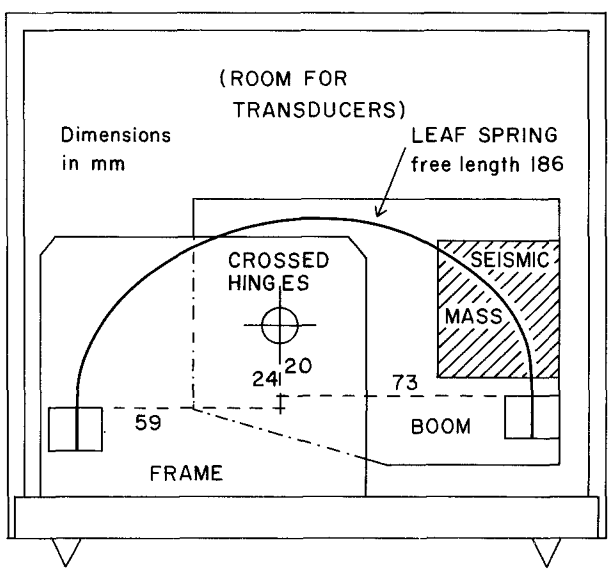

FIG. 5. Spring geometry of the leaf-spring seismometer.

of different material we can theoretically obtain a perfect temperature compensation. However, since the TCs themselves depend on temperature, this will work only in the vicinity of a specified temperature. The operating range of the leaf-spring seismometer is normally from 0 to 30°C. In high gain applications where the LP output signal is dc-amplified before band-pass filtering, the temperature range is reduced according to the gain, and recentering may be necessary after a temperature change of a few degrees. This does not cause any serious problems but must be taken into account in the design of VLP passband filters.

Transducers

The leaf-spring seismometer has three cartridge-shaped transducers mounted horizontally on top of the frame (Figure 2). Two of these are moving-coil electromagnetic transducers and generate the feedback force. They are arranged antiparallel to each other so that second-order terms in the electromagnetic force are cancelled which are expected to occur in a single transducer.

The third transducer is a displacement sensor of the linear variable differential transformer (LVDT)-type. It was especially designed for this seismometer and resolves 10^{-10} m peak-to-peak. Its operating range is 0.5 mm. The LVDT principle was chosen for practical reasons: LVDT transducers are insensitive to environmental conditions and do not require active electronic components inside the vacuum chamber. On the other hand, compared to capacitive transducers, LVDTs have inferior resolution and exert more force on the seismic mass. Quantitative information of these effects is given in the section on "Instrumental Noise." Our test results indicate that the use of a LVDT transducer does not limit the performance of the leaf-spring sensor for any kind of teleseismic recording; however, the displacement resolution is insufficient for microearthquake recording.

The Feedback Circuit

The feedback circuit used with the leaf-spring sensor is of the force-balance type that is now standard in electronic seismometers. Since the force-balance principle has sufficiently been covered in the seismological literature (Melton, 1976; Usher *et al.*, 1978), we shall only summarize the basic results and then discuss some properties of the actual circuit.

The difference between a conventional and a force-balance seismometer can in a simplified way be described as follows. The idea behind a conventional LP seismometer is to measure the motion of the ground against an inertial reference, i.e., against an elastically suspended mass that is supposed to stay at rest when the ground moves. A force-balance system senses the ground motion after the same inertial principle, but provides an additional electrostatic or electromagnetic restoring force that causes the mass to follow the motion of the ground. This principle reduced greatly the relative motion between the mass and the frame and facilitates the mechanical design. As long as the feedback circuit is efficient in keeping the relative motion of the mass small, the driving force is nearly proportional to ground acceleration and nearly independent of the circuit that controls it. The electric voltage or current that generates the force is used as an output signal. The precision to which we are able to measure the ground motion depends essentially on the precision of the force transducer, in the same way as the precision of a potentiometric recorder depends on the quality of the potentiometer. Electromagnetic force transducers can have a much better linearity and dynamic range than any available mechanical suspension or displacement transducer.

Figure 6 is a simplified circuit diagram of our feedback electronics. Three parallel feedback paths are provided: proportional feedback over the resistor R_1, differential feedback over the capacitor C, and integral feedback over the integrator and the resistor R_2. The components have been chosen such that the differential feedback force dominates at periods shorter than 20 sec and the integral force at longer periods. Since the feedback current adjusts itself nearly proportional to ground acceleration, the voltage across the capacitor—i.e., at the BRB output—is nearly proportional to ground velocity up to a 20-sec period. Neglecting the mechanical restoring force and damping of the suspension, the impedance of the feedback coils, and complications arising from the circular motion of the mass, the response $V \exp(i\omega t)$ of the BRB output to a harmonic ground motion $X \exp(i\omega t)$ is obtained as

$$\frac{V}{X} = \frac{i\omega^3 M/\sigma C}{-i\omega^3 M/\alpha\sigma C - \omega^2 + i\omega/R_1 C + 1/\tau R_2 C}.$$

An explanation of the symbols and approximate values of the components are given in Figure 6. Apart from the term with ω^3 in the denominator, this equation represents the transfer function of an electrodynamic seismometer with the angular eigenfrequency $\omega_0' = (\tau C R_2)^{-1/2} \approx 2\pi/20$ sec, the damping constant $h' = (2R_1)^{-1}(\tau R_2/C)^{1/2}$ ≈ 0.71, and the electrodynamic transducer constant $M/\sigma C \approx 2500$ V/m. In fact, the feedback system has been designed to replace a conventional LP seismometer. R_1 has the function of a damping resistor; damping can be removed for test purposes by disconnecting R_1, without changing the other parameters of the system.

The term with ω^3 in the denominator indicates a deviation from the response of a conventional instrument. It becomes significant at periods shorter than 0.2 sec where the loop gain falls below unity. A further deviation results from the resistance of the coil for differential feedback. We can, however, maintain the analogy with conventional equipment if we insert an additional first-order low-pass filter with about a 0.2-sec corner period into the output circuit. The overall response can then be made identical to that of a 20-sec LP seismometer coupled to a 0.2-sec recording galvanometer. We make use of this analogy when we calibrate the feedback system against an electronic standard circuit as described later.

The signal at the LP output is a time integral of the BRB signal and corresponds to the output signal of a conventional LP seismometer with a displacement transducer. This signal is preferably used for acceleration recording in the free-mode

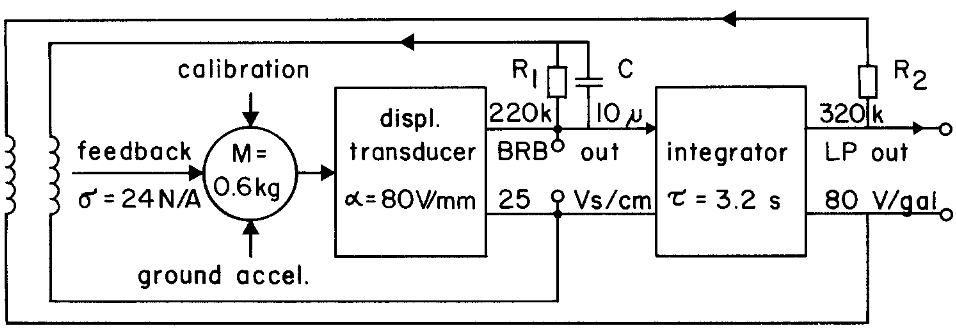

FIG. 6. The feedback circuit.

band but is also useful to record displacement at intermediate periods for magnitude and moment determinations. The low gain of about 800 V/m permits us to observe surface waves of 70 mm peak-to-peak amplitude at a 20-sec period without clipping.

The leaf-spring sensor can as well be operated with the integral feedback disconnected. The response at the BRB output is then proportional to ground velocity at periods shorter than 20 sec and proportional to acceleration at longer periods. The modified system combines the broadband and the LP responses in one output and has a larger dynamic range. However, its response is no longer compatible with that of conventional instruments.

INSTRUMENTAL NOISE

Even if the seismometer is operated under constant environmental conditions and has no mechanical imperfections, four potentially significant sources of intrinsic noise must be considered: (1) the Brownian motion of the mass; (2) the noise of the displacement transducer; (3) the integrator noise; and (4) the noisy component of the electromagnetic force acting on the core of the LVDT. The spectrum of the Brownian noise is white in terms of acceleration, i.e., it has a constant acceleration power density. The other three components result from semi-conductor noise whose power density increases approximately with $1/f$ at low frequencies; such noise has a constant power in frequency bands of equal relative width. The values given below refer to a bandwidth of one sixth of a decade, e.g., to the bands from 100- to 147-sec periods, from 147 to 215 sec, from 215 to 316 sec, etc. Each component of the noise can be expressed as an equivalent ground acceleration. The results are plotted in Figure 7 in terms of spectral power density.

(1) Brownian motion. After Melton (1976) or Usher *et al.* (1978), the Brownian motion of a suspension with the inertial mass M, free period T, and mechanical quality factor Q corresponds to an acceleration power density

$$\bar{\ddot{x}}^2/\Delta f \approx 10^{-19}\ \mathrm{m}^2\ \mathrm{sec}^{-3}/MTQ.$$

By coincidence, the prefactor $10^{-19}\ \mathrm{m}^2\ \mathrm{sec}^{-3}$ is the limit below which the instrumental noise of a VLP sensor can be neglected against the seismic noise; this value forms

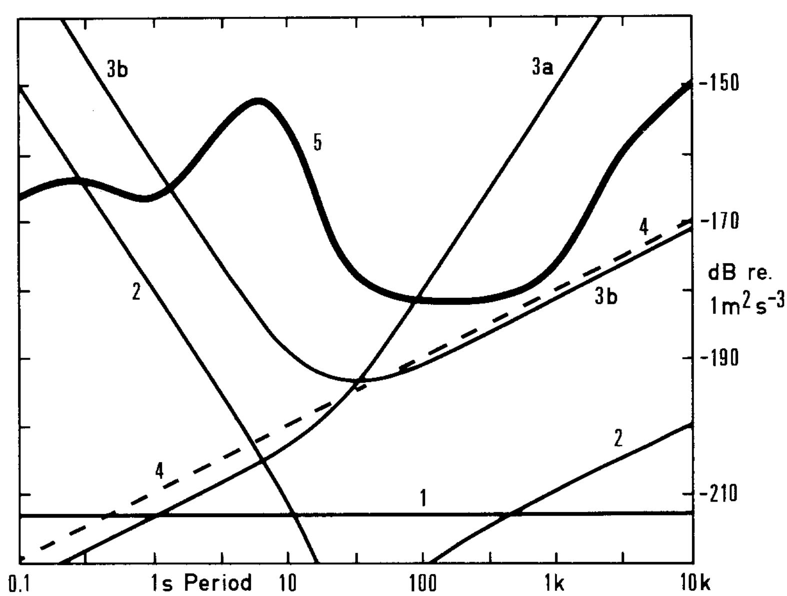

FIG. 7. Intrinsic noise of the leaf-spring seismometer in terms of equivalent ground acceleration (decibles relative to 1 $\mathrm{m}^2\ \mathrm{sec}^{-3}$). (1) Brownian motion, for MTQ = 200 kg sec; (2) displacement noise of the LVDT; (3) integrator noise—(a) BRB output and (b) LP output; (4) electromagnetic force of the LVDT; (5) minimum observed ground noise, compiled from Berckhemer (1970), Agnew and Berger (1978), and Figure 10 of this paper.

the baseline of our Figure 10. A VLP sensor should have $MTQ > 1$ kg sec. The leaf-spring suspension has a MTQ product of several hundred kilogram seconds; its Brownian noise is therefore well below the critical value.

(2) Displacement noise. The transducer has an equivalent noise of 15 pm rms in $\frac{1}{6}$ decade. As is apparent from Figure 7, this noise is of concern only at the short-period end of the seismic spectrum. Most stations have, of course, a much higher short-period noise level than assumed in Figure 7, so the rise in instrumental noise at short periods is in most cases insignificant.

(3) Integrator noise. The equivalent input noise of the integrator is typically 0.1 μV in $\frac{1}{6}$ decade. Its effect is different at the two outputs of the system. The integrator noise is below the seismic noise in the passband of each output, but may become noticeable when the LP output is used at short periods, or the BRB output at very

long periods. The small margin between the seismic noise and the integrator noise at a 400-sec period is a deliberate feature; it can be enlarged at the expense of operating range.

(4) Electromagnetic noise from the LVDT. Due to small deviations from mechanical and electrical symmetry, the LVDT exerts a force in the order of 10^{-5} N (1 dyne) on its movable core. Fluctuations of this force contribute to the instrumental noise. Using a modified seismometer whose spring was removed and whose boom was balanced with respect to the axis of rotation, we determined that the force noise is less then 10^{-11} N rms in $\frac{1}{6}$ decade, corresponding to an acceleration smaller than $2 \cdot 10^{-11}$ m^2 sec^{-3} rms. This is negligible over most of the seismic band except near a 400-sec period where the electromagnetic noise is only a few decibels below the seismic noise. Since the electromagnetic force is proportinal to the square of the AC voltage that excites the LVDT, it will be reduced by a factor of 100 when the primary voltage is reduced by a factor of 10. The original responsivity and resolution can be restored with a preamplifier in the secondary circuit. It is planned to include this modification in future instruments.

Dynamic Range

The dynamic range of a signal processing system is defined as the interval between its noise level and its clipping level. It depends on frequency and on the bandwidth in which the noise is measured. The clipping level at the output is normally determined by the voltage of the power supply while the noise level is within certain limits proportional to the gain. There are two considerations which impose a lower limit to the gain and, thus, an upper limit to the dynamic range. First, the smallest output signal of interest must still be large enough to be recorded. The dynamic range of a feedback system may, therefore, be determined by the filtering and recording facilities available at the time of design rather than by some intrinsic limitations of the feedback circuitry. Second, although the signal-to-noise ratio is as a rule independent of the gain, the noise at the output does not decrease indefinitely with the signal when the gain is reduced. In a closed-loop system, noise generated in the feedback loop excites the mechanical system and appears at the output with an amplitude that is virtually independent of the gain. The dynamic range of a feedback seismometer can be as large as that of its feedback loop. It is presently limited to about 140 dB when the feedback path includes active components, but can be substantially larger when the feedback path is purely passive.

The feedback system of Figure 7 is not purely passive but is predominantly passive if we use the appropriate output at each period. At periods shorter than 20 sec, the passive feedback from the BRB output dominates the active integral feedback. At longer periods, the integral feedback dominates; its path is passive as seen from the LP output. A quantitative analysis based on the noise spectra of Figure 7 shows that the dynamic range exceeds 140 dB for periods between 0.2 and 130 sec at the BRB output, and for periods longer than 5 sec at the LP output. These figures refer to a bandwidth of one-sixth of a decade.

The maximum permitted seismic signals can be determined by dividing the maximum electric signal at each output by the appropriate transfer function. We give only the results here: the system accepts displacements up to ±0.25 mm, velocities up to ±8 mm/sec, and accelerations up to ±2.5 mm/sec^2 (whichever is largest) at any frequency. It would not be saturated by vibrations of ±0.1 *g* at frequencies above 10 Hz. To our knowledge, none of the leaf-spring seismometers installed in Switzerland or in the GRF array has ever been saturated. In contrast, an accelerometer with the same LP response as the LP output of our system would have a clipping level of ±0.00025 *g* at all frequencies, and could easily be saturated by traffic noise or small local earthquakes. Certainly this is one of the reasons why sensitive wideband accelerometers, although technically feasible, have not found wide use for seismic recording.

We illustrate the dynamic range of our instrument with Figure 8 that reproduces a series of playbacks of a digital wideband record of the second strong Friuli earthquake in 1976. Magnifications range from 100 to 600,000 at 1 Hz. New details appear each time the gain is increased. A signal six times stronger could still have been recorded.

LINEARITY

Linearity is essentially for seismometers when weak LP signals must be recorded in the presence of strong short-period noise. Such a situation is quite common since

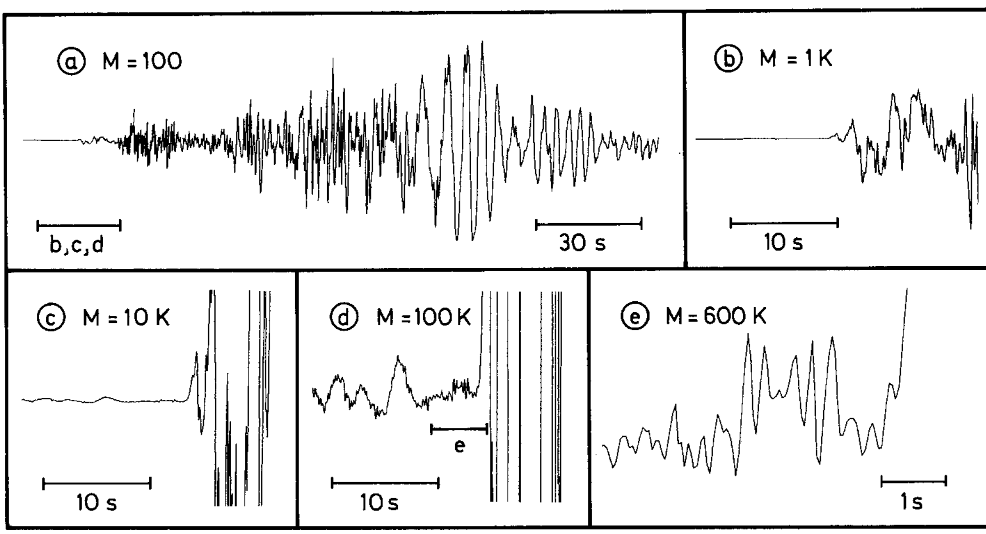

FIG. 8. Playbacks of a digital wideband record of the second large Friuli earthquake 15 September 1976, 09:21 UTC, m_b = 5.4 (USGS, Δ = 400 km). The magnifications *M* refer to the original figure where the peak-to-peak amplitude of trace (a) is 47 mm. (Courtesy of D. Seidl, GRF Observatory.)

marine microseisms and man-made noise can have amplitudes many orders of magnitude larger than LP seismic signals, especially when measured as an acceleration. A nonlinear system would convert amplitude variations of short-period signals into spurious LP signals. Block and Moore (1966) mention that the sensitivity of their LaCoste-Romberg gravimeter system in the free-mode band was most probably limited by its nonlinear response to short-period signals.

The linearity of a system can be tested by applying two sinusoidal signals of equal amplitude and nearly equal frequency to the input and observing their low-frequency intermodulation products at the output. A test procedure for the SRO system based on this method has been described by Peterson *et al.* (1980). Following a suggestion by Jon Peterson, we have subjected three of our instruments to the same test. When the input signal drives the instrument through half of its operating range, the distortions at the output are typically 80 dB below the signal or 0.005 per cent of the operating range. This is comparable to the distortion level in the SRO seismometer but indicates a substantial difference between the two systems: our instruments were, according to their greater operating range, tested with a signal of 50 mm/sec^2 peak-to-peak, which is 2300 times stronger than used for the SRO system.

Figure 9 is another illustration of the linearity of the leaf-spring system. It shows the VLP signals recorded at Zürich during three local magnitude 4 earthquakes, and a 6 μgal calibration pulse for comparison. The events occur in the center of each trace; the short-period seismic signals are suppressed by the VLP passband filter. Only a single, very slight deflection barely above the background noise appears in each trace, even after the third event, one felt at Zürich. It is possible that these deflections indicate LP components of the seismic signal; we suspect, however, that they are due to a small nonlinearity in the VLP passband filter.

Measurements of VLP Ground Noise

We have obtained a great number of LP noise spectra with the prototype leaf-spring seismometer which is installed in a vault next to the building of the Institute of Geophysics of ETH Zürich. (A 40-m thick layer of postglacial sediments makes the site unattractive for short-period recording.) Most of the spectra were computed on-line with a digital spectral analyzer. The noise samples were in a few cases up to 240,000 sec long when the teleseismic activity permitted. Our results are represented

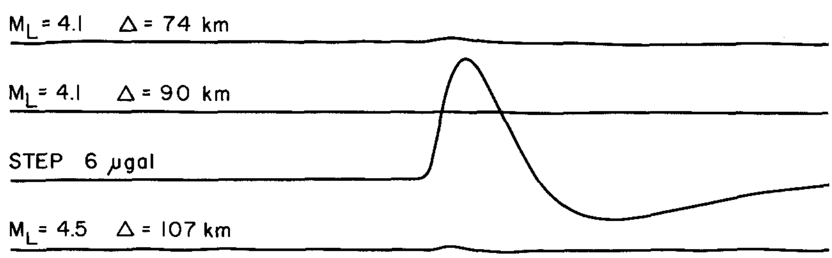

FIG. 9. Response of the VLP trace to three regional magnitude 4 earthquakes. Time interval shown is 10 min before and 10 min after each event. The third trace shows a calibration pulse. The earthquakes were: 26 March 1976, at 22:28 UTC; 2 September 1977 at 22:47 UTC; 16 January 1978 at 14:31 UTC; all in southwest Germany.

in Figure 10 by a hatched band into which about 90 per cent of all individual observations fall. The noise power density has been smoothed over a constant relative bandwidth of one-sixth decade.

Our observations are in remarkable agreement with those of Agnew and Berger (1978; dotted line in Figure 10) and permit two conclusions.

1. The vertical VLP ground noise at Zürich is not larger than at the best IDA stations.
2. The leaf-spring seismometer does in fact resolve ground noise in the free-mode band as predicted by Figure 7.

The formal alternative—that ground noise at Zürich is lower than anywhere else but is not resolved—appears fairly remote.

A partial confirmation was obtained from a cross-spectral analysis between the output signals of the prototype sensor and a newly manufactured instrument. The correlation between the signals was good up to a 500-sec period. At longer periods, the new instrument showed a slightly elevated noise level due to small transient disturbances in its output signal. We observe these in most new instruments. They have an amplitude of about 100 ngal, initially occur every few hours, and usually disappear within 1 yr in a permanent installation. In any case, the transients are so small that they are barely seen in a high-gain VLP record, and never in a normal LP record. It is not clear from which part of the seismometer they originate; we suspect that stresses in the mechanically overdetermined frame may be responsible. Recently introduced modifications in the manufacture of the frame appear to have substantially reduced the occurrence of such disturbances.

CALIBRATION

When the transfer function of a seismometer is sufficiently stable, as is the case for a properly designed feedback seismometer, it need be calibrated only once after manufacture. This can save much tedious work during the installation where convenient test equipment is often not available. We describe the essential steps of the calibration of a leaf-spring seismometer; most of these can equally be applied to other force-balance seismometers.

Mechanical adjustments. After manufacture, the mechanical system is adjusted such that: (i) the linear trend of the free period is minimized over the range of the displacement transducer; (ii) the sensitive axis is precisely vertical; (iii) the free

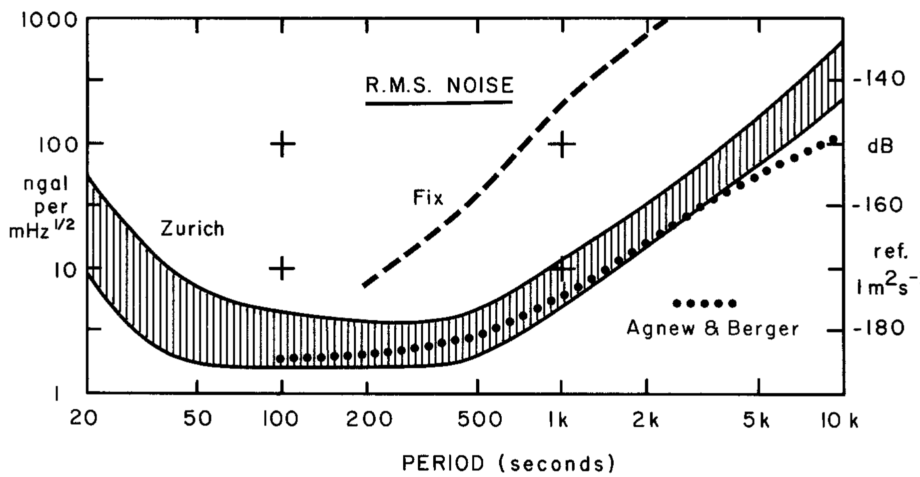

FIG. 10. LP seismic noise, including instrumental components, expressed as acceleration power density relative to 1 m^2 sec^{-3} (right-hand scale). Broken line, after Fix (1972); dotted line, after Agnew and Berger (1978); *hatched band*, observations with the leaf-spring seismometer at Zürich.

period is virtually infinite. These three steps require repetitive adjustments of the length and position of the spring, the size and position of the seismic mass, and the neutral position of the displacement transducer. The spring is adjusted after computer-generated diagrams that describe the influence of small changes in the clamp position on the free period. The sensitive axis is vertical when the sensor indicates maximum gravity on a tilt table, as described below.

Feedback system. The transfer function at the BRB output is calibrated against an electronic reference circuit that simulates a 20-sec seismometer coupled to a 0.2-sec glavanometer (the reason for this choice has been mentioned above). The comparison is made by means of an X-Y plotter that plots the difference between the two output signals versus the input signal when the seismometer and the reference circuit are excited with the same sine wave. The Lissajous figure does not only indicate calibration errors but also nonlinear distortions if present. The feedback components are adjusted until a satisfactory agreement with the reference circuit is obtained over the whole passband. Residual errors in the phase delay are normally less than 5 msec or 0.001 of the signal period whatever is larger. Errors five times as large may be caused by transportation, installation under different conditions, and aging; this is still a better precision than most conventional LP seismometers would have when calibrated after installation. The LP output does not require a separate calibration because it delivers simply the integrated BRB signal.

Absolute calibration. Gravity is used as a reference to calibrate the absolute gain of the LP output at zero frequency. The sensor is put on a tilt table and the voltage at the LP output monitored as a function of the tilt angle. When the sensor is tilted by an angle φ against the vertical, it responds only to the component $g_0 \cos\varphi$ of the gravity g_0. The responsivity to accelertion at zero frequency is determined by forming second-order differences of the output voltage $V(\varphi)$ with respect to φ

$$\frac{\Delta V}{\Delta g} = -\frac{1}{g_0}\frac{\Delta^2 V}{\Delta\varphi^2}.$$

Horizontal seismometers are calibrated in a similar way but this time first-order differences are evaluated

$$\frac{\Delta V}{\Delta g} = \frac{1}{g_0}\frac{\Delta V}{\Delta g}.$$

We estimate that the precision of the absolute calibration is better than 1 per cent; the agreement with shake table experiments is also within this margin.

Installation. The only adjustment that remains to be done at the time of installation is to bring the sensor again into that position with respect to the vertical in which it was during calibration. While the geometrically well-defined transverse axis can be adjusted with a bubble level, this is in general not possible with the longitudinal axis because it is not geometrically determined. We level it using the restoring force of the suspension as an indicator. Due to the previous mechanical adjustments, the restoring force disappears in the correct position. To monitor the restoring force, we disconnect R_1 (Figure 6) and observe the free oscillations of the closed-loop system at a period of 20 sec. A positive mechanical restoring force has the same effect as a negative proportional feedback, i.e., it damps the closed-loop oscillations. Thus, a constant amplitude of these oscillations indicates that we have found the correct position. The procedure may appear complicated in theory but is very convenient in practice. A precise alignment of the vertical axis is important not only for the transfer function but also because a misadjusted vertical sensor would respond to horizontal ground noise and not reach its full resolution.

LP Responses

In this chapter we collect some information on four LP responses that have been realized with the leaf-spring sensor and visible recording. This is, of course, not the latest technology but still an economic one for specific applications. The need to shape the response with analog filters is eliminated when digital wideband recording is available, any desired response can later be obtained by digital filtering (Harjes and Seidl, 1978; Seidl, 1980). Figure 11 illustrates the usefulness of the wideband concept: it shows an original SRO-LPZ record from GRFO and filtered wideband data from a leaf-spring seismometer in a surface installation at the same site. Not only the signal but also the noise is identical in both traces.

The gain of a conventional LP seismograph is normally limited by microseismic and environmental noise, and its response is not sufficiently flexible to be adapted to specific problems. These limitations do not exist for electronic seismographs. So, if we still realize standard responses with these, it is for compatibility with existing equipment which is often more important than technical sophistication. Alternatively, we may either wish to make the response inverse to the spectrum of a typical signal (for analysis), or inverse to the spectral distribution of ground noise (for detection, or find some compromise between these two ideas. Table 1 contains one example for each of the four cases, in that order. The resulting magnification curves are given in Figure 12.

A standard WWSSN-LP response is realized with the leaf-spring seismometer as with any other LP seismometer by using a LP amplifier-filter circuit such as described by Wielandt and Mitronovas (1976). The chopper preamplifier of that circuit may be omitted in connection with the leaf-spring seismometer. The velocity

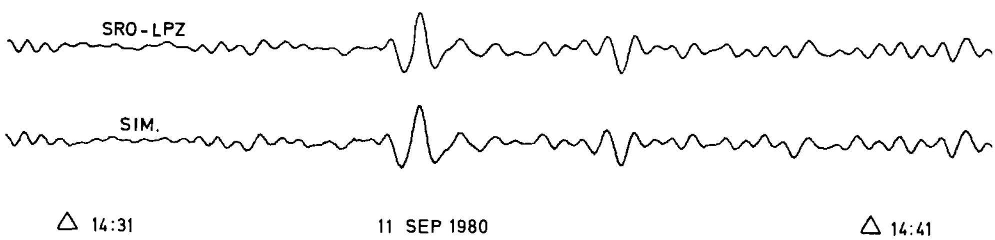

FIG. 11. Original and simulated SRO-LP records of a distant event (11 September 1980 at 14:14 UTC; $m_b = 5.2$, $\Delta = 125°$). Original magnification is 33k at 20 sec. (Courtesy of D. Seidl, GRF Observatory.)

TABLE 1

SUGGESTED LP RESPONSES*

Response	LP Velocity	LP Displacement	Narrowband LP	VLP Accceleration
Flat from (sec)	20	20	30	200
To (sec)	90–300	90–300	90	600–3000
Seismometer output	BB	LP	LP	LP
High-pass filter	None	300	90	600–3000
Low-pass filter	90–300	90–300	30 (6th order)	60 and 200
Elevation gain (×1000)	3.8–42	3.8–42	9.3	35
Magnification	1k at 20 sec	1.4k	20k at 30 sec	2.4k at 120 sec
Limited by ground noise at	5–8 sec	6–10 sec, VLP	18–20 sec	VLP
Paper speed (mm/sec)	30	30	3	12

* Corner periods are given in seconds. Filters are second-order Butterworth unless otherwise noted. Gains and magnifications refer to a chart recorder with a deflection of 1 cm/V. With the gain indicated, typical ground noise is just visible in the record. Larger gains may be useful for detection.

response can be made flat up to a 300-sec period if desired, without altering the response in the standard passband.

A response flat to displacement in the LP band results when the LP output of the leaf-spring seismometer, in place of the BRB output, is connected to the same LP amplifier as in the first case. Such a system records Rayleigh waves from earthquakes around magnitude 6 with approximately equal amplitudes over a wide range of periods, up to the corner period specified. The maximum corner period is 300 sec due to the presence of VLP ground noise; only at the expense of magnification we would be able to extend the flat displacement response further.

The narrowband, LP response of Table 1 is comparable to the response of the HGLP network, and the SRO-LP response. All of these are approximately inverse to the spectral distribution of ground noise in the LP band and have a high gain to make the noise visible. This is good for detection but makes the system susceptible to saturation. Also, signal components with 20- to 30-sec periods, particularly surface waves, dominate so strongly in the records that other components of the signal may be difficult to evaluate. As a typical narrowband, LP seismogram we reproduce in

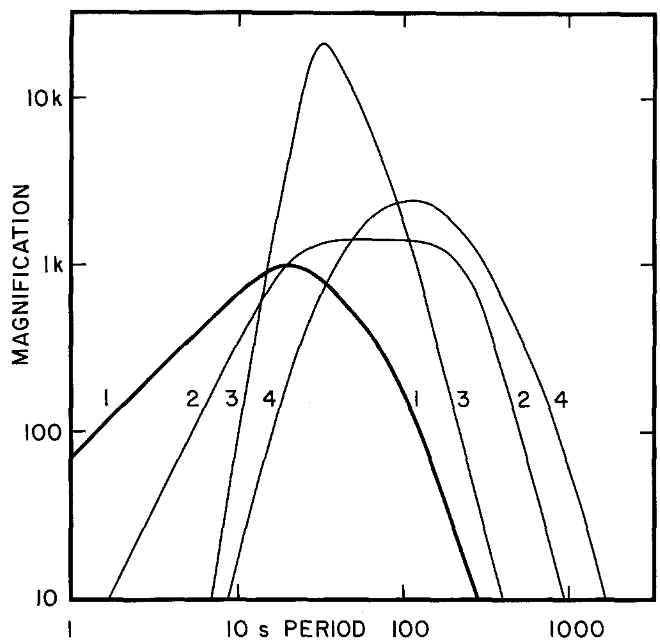

FIG. 12. Magnification curves for the four LP responses of Table 2. (1) LP velocity 20 to 90 sec (close to standard LP); (2) LP displacement 20 to 240 sec; (3) high-gain, narrowband LP (analogous to HGLP and SRO-LP); (4) VLP, 200 to 850 sec.

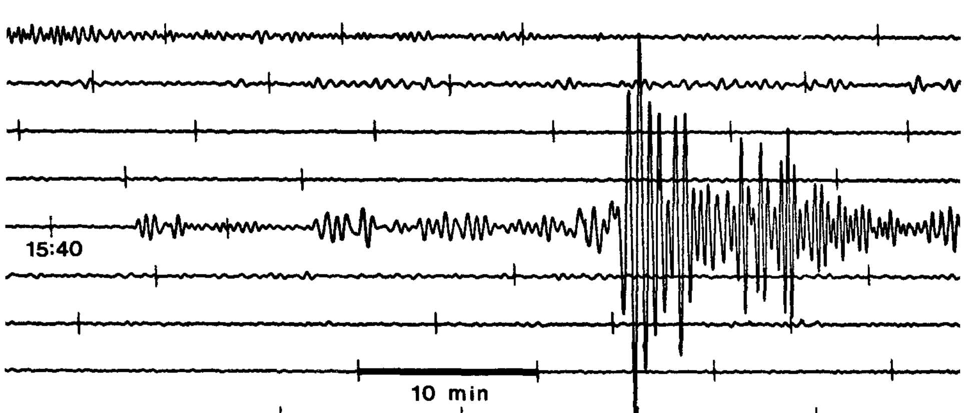

FIG. 13. Mount St. Helens' explosion recorded at Zürich with the narrowband LP system, 18 May 1980, 15:33 UTC.

Figure 13 the signal recorded at Zurich from the explosion of Mount St. Helens in May 1980.

When we try to reduce marine microseisms to an insignificant level, to fit the response to the spectrum of a typical surface wave train at periods up to about 240 sec, and that of the ground noise at longer periods, we arrive at the VLP response of Table 1. It is comparable to the response of other VLP systems such as described by Agnew *et al.* (1976) and Nakanishi *et al.* (1976). A corner period of the high-pass filter around 600 sec would be adequate for visible recording and one up to 3000 sec for digital recording. Even with visible recording and subsequent digitization, we have observed spheroidal free oscillations as low as ${}_0S_4$ (T = 1546 sec), and also

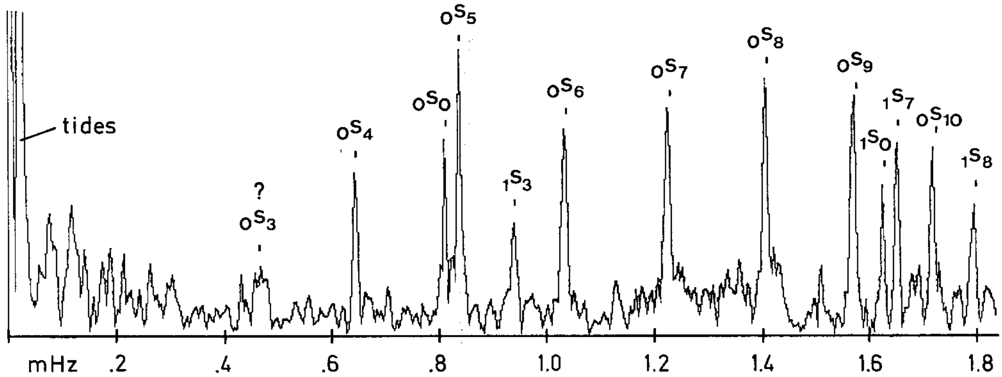

FIG. 14. Free-mode spectrum observed after the Sumba earthquake of 19 August 1977, 6:09 UTC. Fifty-one hours of data, beginning 51 hr after the event, were analyzed. The amplitude of mode ${}_0S_0$ is ±10 ngal or about ±0.1 mm in the VLP paper record (Figures 12 to 14).

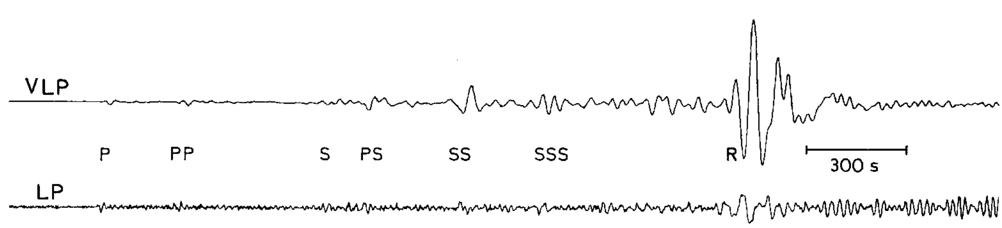

FIG. 15. LP and VLP records of an m_b = 5.2 event at 96° distance (Peru, 28 February 1981 at 21:56 UTC). The event can barely be identified in short-period records.

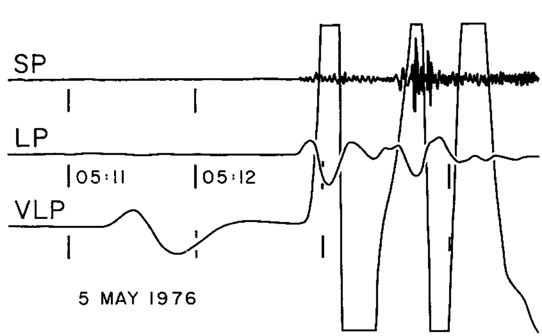

FIG. 16. Short-period, LP, and VLP arrivals from an earthquake at 162° distance (Kermadec, 5 May 1976, 04:53 UTC, m_b = 6.2). Amplitudes are not to scale.

mode ${}_0S_0$ (T = 1228 sec), after the Indonesian earthquake of 1977 (Figure 14). The on-line spectral analyzer reveals spheroidal modes down to ${}_0S_7$ (T = 812 sec) after most magnitude 7 earthquakes.

Figures 15 and 16 demonstrate the difference between a conventional LP record and a VLP record. The earthquake in Figure 15 was an event with m_b = 5.2 at 96°

distance. The LP record would not be considered for a dispersion analysis; however the VLP record clearly shows the inversely dispersed branch of the Rayleigh wave train up to about a 240-sec period, potentially providing information on the shear-wave velocity in the mantle down to 500-km depth. Figure 16 compares the short-period, LP and VLP *P*-wave arrivals from a magnitude 6.2 earthquake in the Kermadec region, at 162° distance from Zurich. The *P* wave diffracted along the core-mantle boundary appears in remarkable clarity in the VLP trace, at an epicentral distance where it is rarely seen on standard LP seismograms.

Acknowledgments

It is a pleasure to acknowledge stimulating discussions with Drs. A. Plešinger, E. Unterreitmeier, W. Zürn, and Professor H. Berckhemer. Test results were made available by Drs. H.-P. Harjes and D. Seidl (GRF Observatory), W. Zürn (Black Forest Observatory), and Mr. J. F. Fels (IPG Paris).

E. Wielandt was supported by the Institute of Geophysics, Swiss Federal Institute of Technology, Contribution No. 376.

References

Agnew, D. C. and J. Berger (1978). Vertical seismic noise at very low frequencies, *J. Geophys. Res.* **83,** 5420–5424.

Agnew, D. C., J. Berger, R. Buland, W. Farrell, and F. Gilbert (1976). International deployment of accelerometers: a network for very long-period seismology, *EOS* **57,** 180–188.

Berckhemer, H. (1970). The concept of wide band seismometry, *Comm. Roy. Obs. Belg., Ser. A No. 13, Ser. Geophys. No. 1,* 1–7.

Block, B. and R. D. Moore (1966). Measurements in the earth mode frequency range by an electrostatic sensing and feedback gravimeter, *J. Geophys. Res.* **71,** 4361–4375.

Block, B. and R. D. Moore (1970). Tidal to seismic frequency investigations with a quartz accelerometer of new geometry, *J. Geophys. Res.* **75,** 1493–1505.

Born, M. (1906). Stabilitaet der elastischen Linie in Ebene und Raum, *Ph.D. Thesis,* Univ. Goettingen (Reprinted in: Max Born, *Ausgewaehlte Abhandlungen,* vol. 1, Vandenhoek und Ruprecht, Goettingen, 1963.)

Fix, J. E. (1972). Ambient earth motion in the period range from 0.1 to 2560 sec, *Bull. Seism. Soc. Am.* **62,** 1753–1760.

Fix, J. E. (1973). Theoretical and observed noise in a high-sensitivity long-period seismograph, *Bull. Seism. Soc. Am.* **63,** 1979–1998.

Galitzin, B. (1914). *Vorlesungen ueber Seismometrie,* B. G. Teubner, Verlag, Leipzig, 1914.

Harjes, H.-P. and D. Seidel (1978). Digital recording and analysis of broad-band seismic data at the Graefenberg (GRF) array.

Jacoby, H.-D. (1971). Die Entwicklung eines kleinen Seismometers mit breitbandigem Ausgangssignal, *Ph.D. Thesis,* Univ. Stuttgart.

LaCoste, L. J. B. (1934). A new type long period seismograph, *Physics* **5,** 178–180.

Melton, B. S. (1976). The sensitivity and dynamic range of inertial seismographs, *Rev. Geophys.* **14,** 93–116.

Melton, B. S. (1981). Earthquake seismograph development: a modern history—Part 1, *EOS* **62,** 505–510.

Melton, B. S. and B. M. Kirkpatrick (1970). The symmetrical triaxial seismometer—Its design for application to long-period seismometry, *Bull. Seism. Soc. Am.* **60,** 717–739.

Milne, J. (1888). The Gray-Milne seismograph, *Trans. Seism. Soc. Japan* **12,** 33–48.

Nakanishi, K. K., L. Knopoff, and L. B. Slichter (1976). Observation of Rayleigh wave dispersion at very long periods, *J. Geophys. Res.* **81,** 4417–4421.

Peterson, J., H. M. Butler, L. G. Holcomb, and C. R. Hutt (1976). The Seismic Research Observatory, *Bull. Seism. Soc. Am.* **66,** 2049–2068.

Peterson, J., C. R. Hutt, and L. G. Holcomb (1980). Test and calibration of the Seismic Research Observatory, *U.S. Geol. Surv., Open-File Rept. 80–187.*

Savino, J. M., *et al.* (1972). Results from the high-gain long-period seismograph experiment, *Geophys. J.* **31,** 179–203.

Seidl, D. (1980). The simulation problem for broad-band seismograms, *J. Geophys.* **48,** 84–93.

Unterreitmeier, E. (1974). Zur Erhoehung der Stoerfreiheit langperiodischer Seismographen-systeme, *Ph.D. Thesis,* Univ. Jena. (Veroeff, Zentralinst., Physik der Erde, Potsdam, 1973.)

Unterreitmeier, E., Ch. Teupser, and H. Buder (1978). Der elektronische Seismograph EDS-1, *Gerlands Beitr. Geophysik* **87,** 441-454.

Usher, M. J., C. Guralp, and R. F. Burch (1978). The design of miniature wideband seismometers, *Geophys. J.* **55,** 605-613.

Warburton, R. and J. Goodkind (1977). The influence of barometric-pressure variations on gravity, *Geophys. J.* **48,** 281-292.

Wielandt, E. (1973). Noise in electronic seismograph systems, *Zeits. Geophysik* **39,** 597-602.

Wielandt, E. (1976). Ein astasiertes vertikalpendel mit tragender Blattfeder, *J. Geophys.* **41,** 545-547.

Wielandt, E. and W. Mitronovas (1975). New developments in long period seismometry, Proc. XIV. Gen. Assoc. ESC, Trieste, 1974, H. Stiller, Editor, Acad. Sci. GDR, Berlin.

Wielandt, E. and W. Mitronovas (1976). An electronic long-period seismograph for surface wave dispersion studies, *Bull. Seism. Soc. Am.* **66,** 987-996.

Willmore, P. L. (1966). Long-period vertical seismograph, U.S. Patent No. 3.292.145.

Eidgenossische Technische Hochschule
Institut fur Geophysik
ETH-Honggerberg
CH-8093 Zürich, Switzerland

Manuscript received 28 December 1981